Transport masses in strained silicon MOSFETs with different channel orientations

D. Rideau*, M. Feraille*, M. Michaillat*, C. Tavernier*, and H. Jaouen*
*STMicroelectronics, 850, rue J. Monnet, FR 38926 Crolles.
Email: denis.rideau@st.com

***Abstract*—The confined states in [001]-oriented strained silicon layers embedded in oxide are investigated using 'full-zone' $k.p$ analysis within the envelop function approximation and Tight-Binding (TB) model. Calculations of important transport parameters - energy band shifts and transport masses - show new results, rising the issues of the limit of simple models like the Effective Mass Approximation (EMA).**

I. Introduction

Uniaxial stress engineering is a key technology to improve MOSFETs performance [1]. When modeling the electrical currents of such devices, it is required to take into account the fundamental carrier transport properties (such as the transport curvature masses and the energy gaps) that are governed by the structure of the 2D electronic energy dispersion relation. The 'full-band' semi-empirical methods, such as the LCBB [2] [3] [4], the Tight-Binding method (TB) [5] and the 30-level $k.p$ -Schrodinger [4] [6] methods are well suitable for the calculation of the confined states in a 2-D gas, but require in general large computer resources. For that reason, most of the mobility calculations available so far in strained nMOSFETs rely on a two step procedure: in a first step the band offsets and the curvature masses are calculated using stress-dependent 3D bandstructure model and in a second step the usual one-band-Schrodinger equation is solved in order to obtain the confined states energy [1]. In this paper, we report on the validity of this approach in Fully Depleted (FD) [001]-Silicon-on-insulator nMOSFETs. Several cases are studied, including channel orientation, electric field, layer thickness, and eventually uniaxial stress.

II. Computational methods

A. Luttinger-Kohn envelop function approximation

In the Luttinger-Kohn envelop function approximation [7] (EFA) the electronic states of the nanostructure are expanded in terms of the Γ-centered Bloch functions of the underlying bulk semiconductor. In case of one-material approximation [6], the $k.p$ -EFA leads to 'multi-band' $k.p$ -Schrodinger-like equations [6], which can be compared in a straightforward way to the usual one-band-Schrodinger equation. Indeed the same algorithm can be used with two different bulk models:

(i) **EMA**: The one band Effective Mass Approximation for electrons that depends on a quantization mass m_z [8].

(ii) **Full-Zone $k.p$ model [9]**: The 30-bands $k.p$ model [9] that accounts for the conduction bands, but also for the valence bands.

In the present calculations, the wave functions are expanded in terms of trigonometric functions, which is an efficient way to solve the $k.p$ -Schrodinger equation [6]. In FD MOSFETs, the Si layer is embedded in oxide and the electronic states are confined in the layer by large Si/SiO_2 band offsets. Within the one-material approximation the confinement in the Si layer can be obtained using an additional positive (negative) potential $V_C = 3eV$ ($V_B = -4eV$) for the Conduction Bands (CB) (and the Valence Bands) at the Si/SiO_2 interfaces.

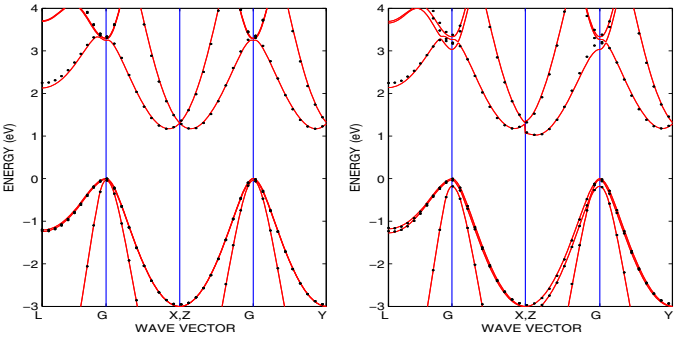

(a) Bulk Silicon.

(b) Uniaxially strained Silicon with 3GPa stress applied along the $< 110 >$ direction.

Fig. 1: Silicon dispersion relation along high symmetry lines in reciprocal space: Tight-Binding (lines), $k.p$ (dots).

B. Tight Binding model

We now discuss a TB method for modeling thin and strained silicon layers embedded in oxide. Our main goal is to compare the solution from such an atomistic technique with those of EMA, and full-zone $k.p$ model within the framework of the envelope-function. The first nearest neighbors $sp^3d^5s^*$ model is one of the most accurate and efficient TB description of semiconductor materials[10]. However, to perform a meaningful comparison with the results of the full-zone $k.p$ -Schrodinger equation, the dispersion relations obtained with theses two models should match as close as possible in bulk Si, but also in strained Si. We used the new parametrization and strain model detailed in Ref. [11]. The model parameters have been *fitted* on reference abinitio Density-Functional Theory simulations following an optimization strategy similar to the one we used in the $k.p$ model [9]. A very close agreement between both models is obtained (as it is testified in Fig. 1) in terms of effective masses at valleys minima [12] and

978-1-4244-1753-7/08/$25.00 ©2008 IEEE

deformation potentials, but also concerning the overall shape of the electronic energy dispersion (even at high energy or in a strained crystal).

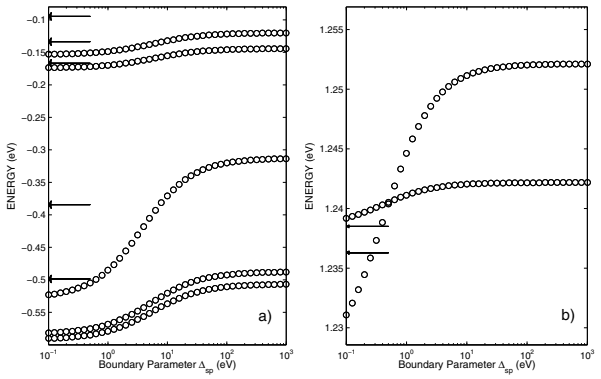

Fig. 2: Sub-bands energy shifts of a [001]-oriented 2nm-thick relaxed silicon layer as a function of the boundary condition a) Valence bands, b) Conduction bands. The parameter $\boldsymbol{\Delta_{sp}}$ is the dangling-bond energy of the surface atoms (see text for details). The arrows shows the sub-bands energy values when the dangling bonds are connected to hydrogen atoms.

In the TB description of the layer, each atom of the silicon crystal is considered and connected to its four neighbors, except at the surfaces. Many surface states in the middle of the gap are present unless passivation of these dangling bonds. An efficient treatment of the surfaces states can be performed by raising the energy of an hybridized orbital [13]. It is also possible to connect these surface atoms to monovalent atoms such as Hydrogen [5]. When the core Si layer is surrounded by a large buffer (e.g. SiO_2) the states are bond in the active layer and are not impacted in principle by the numerical treatment of the surfaces. The authors would like to emphasize that it is not the case, when the dangling bonds at the surfaces of the Si layer are directly passived by one of these techniques. Fig. 2 shows the highest valence-sub-bands and the lowest conduction-sub-bands energies at $\boldsymbol{\Gamma}$ in a 2nm-thick silicon layer as a function of the hybridized orbital energy $\boldsymbol{\Delta_{sp}}$ (see Eq. 4 in Ref. [13]). Also shown in the figure are the sub-bands energy levels obtained with a H-passivation of the dangling bonds. Fig. 2 clearly shows that the energy at $\boldsymbol{\Gamma}$ depends on the passivation model. This behavior is particularly noticeable for the valence bands states. Indeed, interband-coupling induced by the surfaces can significantly modify the holes confined states energy at $\boldsymbol{\Gamma}$ (as well as the overall shape of the dispersion relation -not shown). For electrons, due to larger energy-band gaps, the surfaces-induced interband-coupling seems less pronounced than for holes. It should be noted nevertheless that the energy splitting of the lowest $\boldsymbol{\Delta_z}$ subbands at $\boldsymbol{\Gamma}$, which is known as valley splitting [14], can be inferred from the $\boldsymbol{\Delta_z}$-valleys coupling, and thus depend on the passivation model. However, this splitting is small (e.g. in comparison to the thermal energy) and can be neglected for the analysis of electron transport in thin Si layers unless very low temperatures are considered.

For the rest of this paper, because it is mostly focussed on electrons, we will use the hybridized-orbital-passivation model [15], with $\boldsymbol{\Delta_{sp} = 30}$ eV. We believe that this simple approach captures the main features of the Si/SiO_2 interface (confinement due to large band offsets) without introducing additional details such as coupling due to a change of the crystallographic structure at the interface.

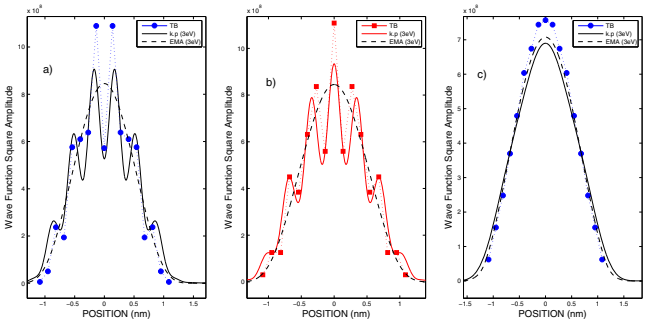

Fig. 3: Electron confined states in a 2 nm-thick Silicon layer: a) wave function square amplitude of the first level at $\boldsymbol{\Gamma}$, b) wave function square amplitude of the second (quasi-degenerate) level at $\boldsymbol{\Gamma}$, and c) wave function square amplitude of the first level at $\boldsymbol{\Delta_x}$.

III. Results and Discussion

A. *Wave function*

Fig. 3 (a,b) shows the wave function square amplitudes for the two lowest quasi-degenerate conduction sub-bands at $\boldsymbol{\Gamma}$ in a 2 nm-thick layer. The TB and $\boldsymbol{k.p}$ models give consistent results. One notes in particular the oscillations of the wave function (whose period is determined by the $\boldsymbol{\Delta_z}$-valleys position along the $\boldsymbol{\Gamma - Z}$ axis), which is not observed with the EMA model. A good agreement between models is found, although the TB wave functions are evaluated at the atoms positions (every $\boldsymbol{a/4}$) only, while the $\boldsymbol{k.p}$ ones exhibit continuous curves along the $\boldsymbol{z}-$direction. Also shown in Fig. 3 (c) are the wave function square amplitudes for the lowest conduction sub-bands at $\boldsymbol{\Delta_x}$-valley minimum. Again, one notes a good agreement between models, although the wave function obtained with the present $\boldsymbol{k.p}$ model extends slightly more outside the well than the ones obtained with the two other models. This is consistent with the fact that the $\boldsymbol{k.p}$ subband lowest energy is $\boldsymbol{46}$ meV lower than the TB one (for comparison the EMA energy is $\boldsymbol{16}$ meV larger than the $\boldsymbol{k.p}$ one).

B. *Confined states energy and curvature masses*

Fig. 4 (a) reports the shifts of the three lowest $\boldsymbol{\Delta_z}$-subbands folded in the center of the 2D-Brillouin Zone [2] (for the reason mentioned previously the valley-splitting is neglected) and $\boldsymbol{\Delta_{x,y}}$-subbands minima as a function of the layer width. As shown the EMA results superimpose very well with the $\boldsymbol{k.p}$ ones (not shown are the TB results that are also in very

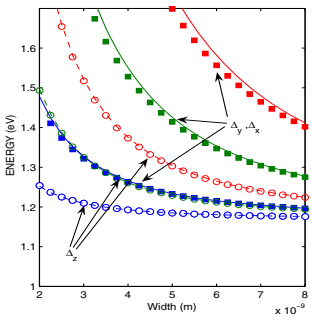

(a) Shifts of the three lowest $\boldsymbol{\Delta_z}$-subbands (o) and $\boldsymbol{\Delta_{x,y}}$-subbands minima (■); 30-level $\boldsymbol{k.p}$ (symbols) and EMA (lines).

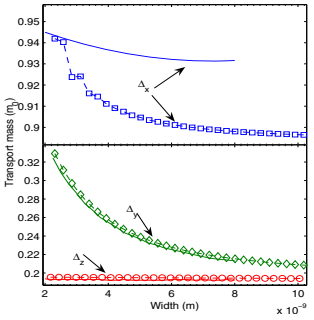

(b) Transport masses along the $< \mathbf{100} >$ direction; 30-level $\boldsymbol{k.p}$ (lines) and TB (symbols) models.

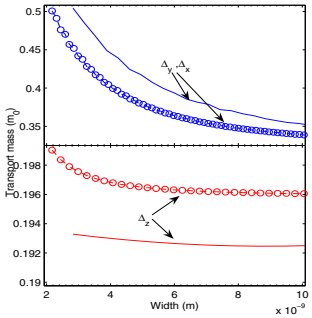

(c) Transport masses along the $< \mathbf{110} >$ direction; 30-level $\boldsymbol{k.p}$ (lines) and TB (symbols) models.

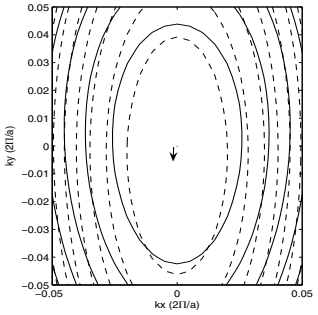

(d) $\boldsymbol{\Delta_y}$ valley first subband energy plots of a 10nm layer (dashed lines) and a 2nm layer (solid lines). The arrow highlights the shift of the ellipsoid.

Fig. 4: The conduction subband energy (a) and transport masses (b,c) as a function of the width of the silicon [001]-layer and typical distortions of the lowest $\boldsymbol{\Delta_y}$ valley 2D-subband energy dispersion relation (d). The zero-energy is taken at the valley minimum, and the equi-energy contour plots are spaced by 10meV.

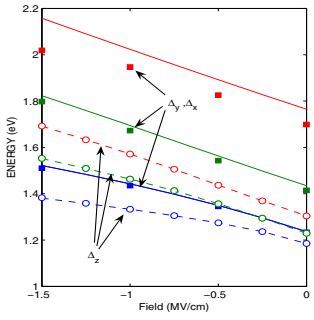

(a) Shifts of the CB subbands minima as a function of electric field values; 30-level $\boldsymbol{k.p}$ (symbols) and EMA (lines).

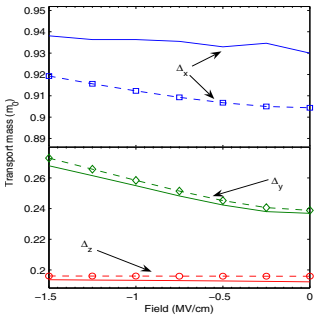

(b) Transport masses along the $< \mathbf{100} >$ direction; same notations as for Fig.1.b.

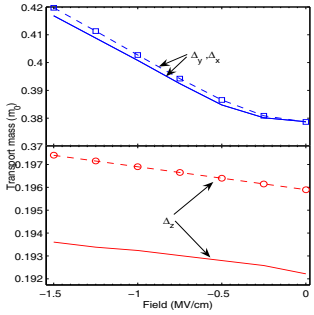

(c) Transport masses along the $< \mathbf{110} >$ direction; same notations as for Fig.1.c.

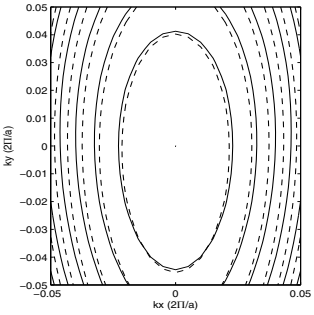

(d) $\boldsymbol{\Delta_y}$ valley energy plots of a 5nm thick layer without (dashed lines) and with an electric field of 1.5MV/cm (solid lines).

Fig. 5: The field-dependent conduction subband energy and transport masses of a 5nm thick silicon [001]-layer, and typical distortions of the lowest $\boldsymbol{\Delta_y}$ valley 2D-subband energy dispersion relation.

good agreement with the $\boldsymbol{k.p}$ ones, specially for the lowest energies). As it will be highlighted during the conference (and already reported in a previous study [4]) this is not the case in ultra-thin [001]-Germanium layers. In Ge, the discrepancies between EMA and full-band models can be large due to a significant coupling between the CBs states and the valence bands states. Due to larger gaps in Si, the coupling is less pronounced and the band shifts calculated with EMA are accurate, even in very thin layer (2 nm).

When considering the transport masses along the channel directions, the situation is nevertheless different. As it can be seen in Figs. 4 (b and c) with both TB and $\boldsymbol{k.p}$ models, certain transport masses can significantly increase when decreasing the layer width [3]. It is notably the case with the $\boldsymbol{\Delta_y}$ valleys the structure of which exhibits a large change in highly confined systems (as depicted in Fig 4 (d)).

The influence of an additional constant electric field (triangular well) has been investigated and similar trends have been found. Fig. 5 shows the conduction subband energy (a) and the transport masses (b,c) as a function of an additional constant electric field value. Similarly to the results of Fig. 4, a very good description of the energy shifts with EMA is found although the transport masses can exhibit strong deviations from their bulk values. This is illustrated e.g. in Fig. 5 (d) by the distortions of the lowest $\boldsymbol{\Delta_y}$ valley with the electric field.

C. Impact of uniaxial stress

A recent wafer bending experiment by Uchida et. al. [1] has shown that uniaxial stress can improve the $< \mathbf{110} >$-oriented nMOSFETs performance. For that stress direction, the crystal is sheared ($\boldsymbol{\epsilon_{yz} \neq 0}$), and a large change in energy gaps and masses can be observed (see Fig. 1). In Fig. 6 (a), we have compared the confined states energy in a 5nm uniaxially strained layer worked out with EMA (in which the strain-induced band offsets have been preliminary calculated with the 3D-$\boldsymbol{k.p}$ model [9]) and with the $\boldsymbol{k.p}$ -Schrodinger method. The EMA reproduce fairly well the subbands energy shifts (as shown somewhere else [16], this is not the case in strained pMOSFETs). However, in Figs. 6 (b and c) we can see large changes in transport masses. This effect, is particularly evident for the $\boldsymbol{\Delta_z}$-valley in case of $< \mathbf{110} >$-stress, and distortions of the valley are shown in Fig. 6 (d).

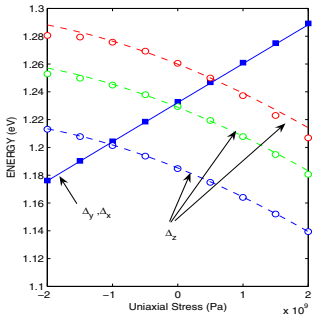

(a) Shifts of the CB subbands minima as a function of uniaxial $< \mathbf{110} >$ strain; 30-level $\boldsymbol{k.p}$ (symbols) and EMA (lines).

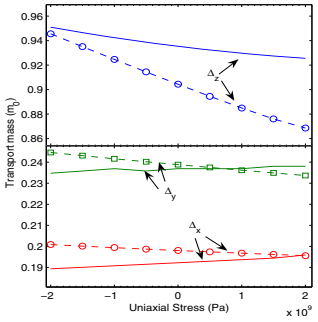

(b) Transport masses along the $< \mathbf{100} >$ direction; same notations as for Fig.1.b.

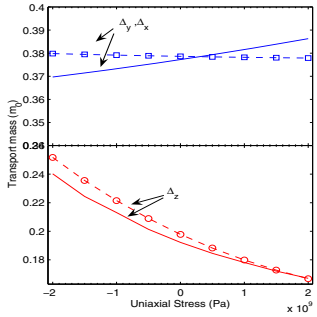

(c) Transport masses along the $< \mathbf{110} >$ direction; same notations as for Fig.1.c.

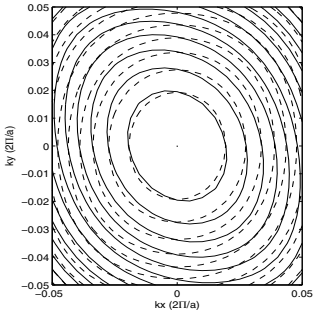

(d) $\boldsymbol{\Delta_z}$ valleys first subband energy plots of a 5nm layer relaxed (dashed lines) and strained with a 2GPa uniaxial $< \mathbf{110} >$ stress (solid lines).

Fig. 6: The strain-dependent conduction subband energy (a), transport masses (b,c), and distortion of the lowest 2D-subband energy dispersion relation in a 5nm thick silicon [001]-layer. The uniaxial stress is applied along the channel direction.

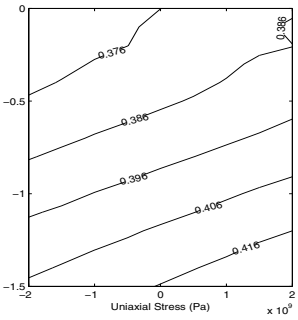

(a) $\boldsymbol{\Delta_{x,y}}$-valleys .

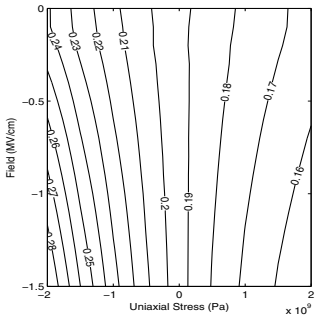

(b) $\boldsymbol{\Delta_z}$-valleys. .

Fig. 7: transport masses along the $< \mathbf{110} >$ direction in a 5 nm-thick layer as a function of electric field and uniaxial stress applied along the channel direction.

To further emphasize the importance of considering the full-band structure of the 2D-system, when evaluating the transport properties in highly confined systems, we have reported in Fig. 7, the transport masses along the $< \mathbf{110} >$-direction as a function of the electric field and the stress values, at the $\boldsymbol{\Delta_{x,y}}$ and $\boldsymbol{\Delta_z}$ subband minima. Simulations have been performed in a 5 nm-thick layer using the 30-level $\boldsymbol{k.p}$ model. One can see that the change in curvature masses exhibits a coupled behavior between strain and confinement. If one focusses e.g. on the $\boldsymbol{\Delta_z}$-valleys, we can clearly see that the way the curvature masses change with strain depends on the electric field value. In absence of electric field, the curvature change in the confined system is roughly identical to the bulk results (results shown in [6]). However, at high electric field (i.e. hight confinement) the change in transport mass due to uniaxial stress is significantly larger than in the bulk case. These latter results show that for highly confined 2D-electrons gas (large electric field or in thin layers ($\boldsymbol{L < 4nm}$) [6]), it can be inaccurate to consider strain and confinement separately.

IV. Conclusion

In this paper we have investigated the validity of the EMA for the calculation of the confined states in strained Si nMOSFETs. To this purpose the $\boldsymbol{k.p}$ -Schrodinger method and the TB model was used to calculate the main parameters that govern the electron density and transport in inversion layers. For the energy shifts at the CB-valleys minima, a good agreement between the predictions of EMA and full band methods is found, even in very thin layers or in strained devices. However, we report large changes (up to 100%) in the transport masses with respect to their bulk values, rising the issues of the limits of the widly used EMA in transport calculations.

Acknowledgment

This work was supported by the French national research agency project "QuantaMonde" (ANR-07-NANO-023-02). Authors are grateful to A. Zaka for a careful reading of this manuscript.

References

[1] K. Uchida et al., Proc. IEDM, 129 (2005).
[2] D. Esseni and P. Palestri, Phys. Rev. B, vol 72, 165342 (2005).
[3] J.P. Van der Steen, IEEE. Trans. Elec. Device, vol 54, 1843 (2007).
[4] D. Rideau *et al.*, Proc. IEEE. SISPAD (2007).
[5] Y. M. Niquet, et al. Phys. Rev. B **62**, 5109 (2000).
[6] D. Rideau *et al.*, submitted to IEEE. Solid State elect. (2008).
[7] J.M. Luttinger and W. Kohn, Phys. Rev. **97**, 869 (1955).
[8] In the $\boldsymbol{\Delta_z}$-valleys, we used $\boldsymbol{m_z = 0.916}$, and in the $\boldsymbol{\Delta_{x,y}}$-valleys we used $\boldsymbol{m_z = 0.1905}$.
[9] D. Rideau *et al.*, Phys. Rev. B, vol 74, 195208 (2006).
[10] J.-M. Jancu *et al.*, Phys. Rev. B **57**, 6493 (1998).
[11] Y. M. Niquet and D. Rideau, submitted to Phys. Rev. B (2008).
[12] In the bulk $\boldsymbol{k.p}$ model: $\boldsymbol{m_l = 0.928}$ and $\boldsymbol{m_t = 0.1925}$ [9] and in the TB model; $\boldsymbol{m_l = 0.89}$ and $\boldsymbol{m_t = 0.1959}$ [11].
[13] S. Lee *et al.*, Proc. 14th Workshop on Modelling and Simulation of Electron Devices, (2003).
[14] M. Friesen *et al.*, Phys. Rev. B 75, 115318 (2007), and references therein.
[15] In a companion study, we have introduced a pseudo-oxide material, acting as a virtual buffer at both sides of the Si layer. The $\boldsymbol{sp^3d^5s^*}$ TB models parameters for this pseudo-oxide material have been chosen in order to obtained Si/$\mathbf{SiO_2}$ band offsets of $\boldsymbol{V_C = 3eV}$ ($\boldsymbol{V_B = -4eV}$) and a direct gap value of 8.17eV. We have compared the results obtained with this model to the ones obtained with $\boldsymbol{\Delta_{sp}}$-passivation of the surfaces. We found for electron only slight differences in terms of energy level and band curvatures at valleys minima.
[16] D. Rideau *et al.*, Proc. ULIS (2008).